

CFD Simulation of the Effects of Extended angle on the Mixing Performances of Rotary Pressure Exchanger

Haiyan Bie^a, Yaping Jia^a, Weizhong An^{a,*}, Chunhong Li^a, Jianmin Zhu^b

^aCollege of Chemistry and Chemical Engineering, Ocean University of China, 238 Songling Road, Qingdao, 266100, China

^bLiaoning Oxiranchem Group, 38 Wanheqi Road, Liaoyang, 111003, China
 awzhong@ouc.edu.cn

By directly contacting with the high and low-pressure fluids, rotary pressure exchanger(RPE) can efficiently recover the high pressure energy of the concentrated salt water and achieve pressure energy transfer, as well as reduce the operation cost of reverse osmosis desalination. Therefore, controlling the radial mixing caused by the direct contact between different fluids is a critical technology for the RPE development to reduce the energy consumption. In this paper, RPE models were built based on the background of reverse osmosis seawater (SWRO) desalination system. On the basis of RPE extended angle concept, the mixing performances of the turbulence model were firstly simulated by CFD software. Then, the structure and operation parameters were changed to analyse the flow field information and reveal the unsteady flow mechanism in RPE. And the flow characteristics of unsteady flow field and the development of high and low-pressure fluid mixing properties in the rotor duct were investigated. The simulation results showed that when the extended angle was $\pm 30^\circ$, smaller volume mixing rate can be obtained compared with no extended angle. The study results can provide a basis for the design and optimization of RPE, and also establish a theoretical guidance for controlling the hydraulic driven rotary device.

1. Introduction

With the rapid development of society and the increasing demand of fresh water resources, seawater reverse osmosis technology has become more and more popular (Tamburini et al., 2016). A rotary pressure exchanger device can efficiently recover the high-pressure energy of concentrated salt water and reduce the running costs of desalination (Elimelech and Phillip, 2011). Therefore, it is widely used in the desalination projects. Liquid energy recycling technology and equipment research have become a hot issue in the field of reverse osmosis desalination. Rotary pressure exchanger core part includes three parts, respectively named the rotor with several channels, the upper and lower stator (Stover, 2004). Because of the direct contact between fresh seawater and high salt water, the energy conversion efficiency is greatly improved (Wu et al., 2015). While it will lead to the two fluids mixed with each other and many other problems. In this regard, many researchers have done a lot of researches on the RPE device (Mei et al., 2012). The two-dimensional numerical model of RPE device was established, and the motion characteristics of liquid column piston in RPE was analysed by CFD technique (Zhou et al., 2009). It was found that the rotor speed and the process flow velocity cancelled each other, therefore the moving distance of the mixing zone kept constant when working conditions had no changes. The influence of operating conditions on the mixing behaviour was studied on the basis of the three-dimensional model (Liu et al., 2012). It was found that the volume mixing rate decreased with the increase of the rotor speed and the decrease of the flow rate. The CFD technology was used to study the effect of the inflow length on the compaction of pressurized seawater, and improved the performance of RPE equipment. It was revealed that the mixing had a polynomial relationship with the dimensionless inflow length, and the conclusion was consistent with the experiment dates (Xu et al., 2014). Based on oscillatory Reynolds number, the mixing features in RPE was simulated using laminar model, and it concluded that the mixing rate was minimized at an oscillatory Reynolds number of about 178 (Cao et al., 2016). Three-dimensional models of the different size and structures in the pressure energy exchanger using the CFD

technology was established to research the performances of the volume mixing rate and the stable time (Wang et al., 2016).

However, the majority of research works used the symmetry model to explore the mixing features of the two fluids. The asymmetric model research has not yet been fully studied. It is not only necessary to reduce the volume mixing of RPE, but also to improve the efficiency of the device in the whole seawater reverse osmosis process. Based on the asymmetric model, the concept of the extended angle was referenced. The influences of the extended angle of the end cover structure on the volume mixing rate and volumetric efficiency were studied by changing the angle of the end cover. The extended angle of 0° , $\pm 30^\circ$ two end cover structures were designed, and the corresponding RPE three-dimensional models were established. The influences of asymmetric structure on the volume mixing rate, volumetric efficiency and NaCl distribution were compared and analyzed.

2. CFD numerical simulation

2.1 Geometric model

Figure 1a shows the three-dimensional geometric model which is built on the basis of the reference and actual device dimensions. Because of its simple structure and meeting the needs of this study, circular channels were used in this paper. The rotor ducts number was set to be 12 to ensure the high and low pressure zones symmetry. The rotor radius was set to be 40 mm, the rotor duct diameter was 15mm, the length of the rotor duct was 150 mm, and the end cover height was 10 mm. Relative to the exit, the inlet had an expansion angle. The angle α and β were defined as extended angles. For convenience, α was set to be positive, and β was set to be negative. The extended angle of $\pm 30^\circ$ was selected in this paper. Figure 1b shows the grid geometry of RPE. Unstructured and structured grids were used to discretize the computational domain. The model included 2,321,952 nodes and 1,920,000 cells. The standard k- ϵ model was used. And it was assumed that no leaks happened. The inlets of the high-pressure brine and the low-pressure fresh seawater were set to be velocity inlets and the inlet speeds of both were set to be 3 m/s. The outlets of the low-pressure brine and the high-pressure fresh seawater were set to be pressure outlets and the outlet pressures were set to be 0.2 MPa and 6 MPa, respectively. The temperature of the brine and fresh seawater was set to be 300 K. In addition, the mass fractions of NaCl of the low-pressure seawater and the high-pressure brine were set to be 3.5% and 6.0%, respectively. To achieve a stable rotation of RPE, the rotor speed was assigned as 1,200 rpm.

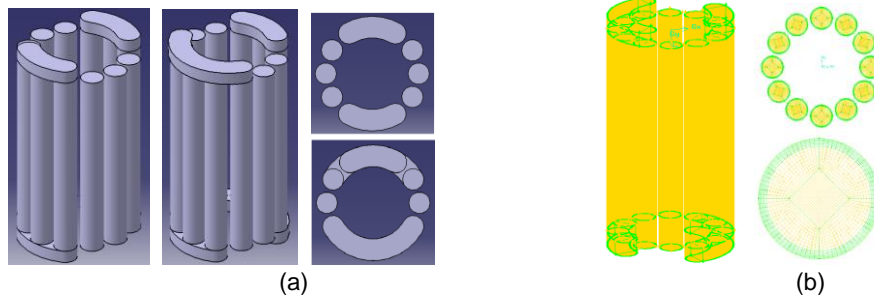


Figure 1: a) Structure diagram of RPE, b) Grid Geometry of RPE.

2.2 Governing equations

The mass conservation equation and the momentum equation are expressed as Eq(1) and Eq(2), and the species transport equation is expressed as Eq(3), where ρ is the density, \vec{v} is the velocity vector, P is the static pressure, τ is the tension tensor, \vec{g} is the gravity constant. Please note that J_i is the mass diffusion flux of species i , which is determined by Fick's law for laminar flows Eq(4), where γ_i is the mass fraction for species i .

$$\frac{\partial \rho}{\partial t} + \nabla \cdot (\rho \vec{v}) = 0 \quad (1)$$

$$\frac{\partial (\rho \vec{v})}{\partial t} + \nabla \cdot (\rho \vec{v} \vec{v}) = -\nabla P + \nabla \cdot (\vec{\tau}) + \rho \vec{g} \quad (2)$$

$$\frac{\partial (\rho \gamma_i)}{\partial t} + \nabla \cdot (\rho \vec{v} \gamma_i) = -\nabla \cdot \vec{J}_i \quad (3)$$

$$\bar{J}_i = - \left(\rho D_i + \frac{\mu_i}{Sc_i} \right) \nabla \gamma_i \quad (4)$$

2.3 Volume mixing rate and Volumetric efficiency

Due to the operating characteristics of the RPE, the pressurized fresh seawater enters the next reverse osmosis seawater desalination system cycle, which will increase the energy consumption. Therefore, it is great important to control the volume mixing rate V_m . V_m is expressed as Eq(5), where S_{HO} is the salinity of the pressurized seawater at high pressure outlet, S_{LI} is the salinity of fresh seawater at low pressure inlet, and S_{HI} represents the salinity of incoming brine at high pressure inlet.

Usually, the maximum inflow length is evaluated as the merits of a rotor design, but it is not enough. Even if a rotor has a large unit cycle processing capacity, but the volume of the whole duct utilization rate is low. The volumetric efficiency η is expressed as Eq(6), where l_{max} the maximum inflow length, l is the duct length.

$$V_m = \frac{S_{HO} - S_{LI}}{S_{HI} - S_{LI}} \quad (5)$$

$$\eta = \frac{l_{max}}{l} \quad (6)$$

3. Results and discussion

3.1 The motion of liquid piston

Figure 2 shows the two-dimensional NaCl distributions of the three-dimensional model of the rotor ducts with a rotational speed of 3 m/s and a rotor speed of 1, 200 rpm at different positions in one rotation cycle. The red parts of the figure represent brine, the blue parts represent fresh seawater, and the rest represents the mixing area. It is seen that the fluid transfer process presents periodic characteristics in the duct, and there is a mixed area of the seawater and the brine in the rotor ducts. The quality of the outlet seawater is affected by the degree of spillage of the mixing area. In a rotation cycle, the liquid piston is done up-and-down reciprocating movement in a single duct, and its reciprocating is a pressure cycle of energy exchange in the duct. In addition, when the rotor goes through a sealed area, it can be seen that the brine is drained from the entire duct and the mixing zone reach the other end of the duct and none overflows out of the duct. The length of the fresh seawater flows into the duct is the maximum inflow length. Similarly, when entering the next sealed area, the fresh sea water is discharged from the duct, and the brine achieves the maximum inflow length. The movement law of the liquid piston is consistent with the results of other researchers.

3.2 Effect of rotor speed on volume mixing rate and volumetric efficiency

Figure 4 shows the NaCl distributions at the same flow velocity of 3 m/s under different rotor speeds. It can be seen that as the rotational speed increases, the contact time between the end cover and the rotor is gradually reduced and the inflow length gradually decreases. According to the analysis of Figure 3, the maximum inflow length of Figure 4a, 4b, 4c, 4d can be obtained. At the beginning of the vertical position of the duct has the high-pressure outlet (pressurized fresh seawater) and low-pressure inlet (fresh seawater). The difference in the mass fraction of NaCl represents, to a certain extent, the degree of mixing of fresh seawater and brine in the high-pressure zone. By changing the rotor speed to explore the performance of RPE, the main parameters include the maximum flow length, volume mixing rate and volumetric efficiency, as presented in Table 1. When the rotor speed increases, the volume mixing rate and volumetric efficiency are decreases. But what may different is the degree of them decrease. The relationships of the volume mixing, the volumetric efficiency and rotor speed are shown in Figure 5. It can be seen that the rotor speeds are inversely proportional to the volume mixing rate and volumetric efficiency. The volume mixing rate and volumetric efficiency decrease with the increasing off the rotor speeds. However, the rotor speeds cannot be too small. As shown in Figure 4a, when the rotor speed is 600 rpm, the mixing parts rush out of the duct. It has great impact on the entire reverse osmosis desalination system. This rotor speed is not suitable to the model constructed in this paper.

Table 1: Main performance parameters of RPE at different rotor speeds.

Speed (rpm)	Maximum inflow length (m)	Volume mixing rate (%)	Volumetric efficiency (%)
600		60	
900	0.097	19.2	64.67
1,200	0.07	12	46
1,500	0.049	4	32.67

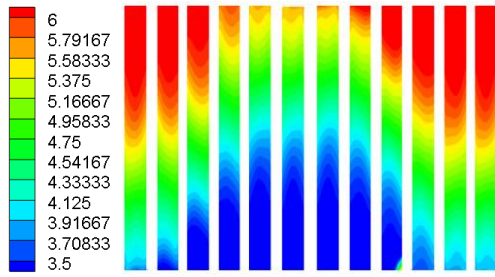


Figure 2: The motion of liquid piston.

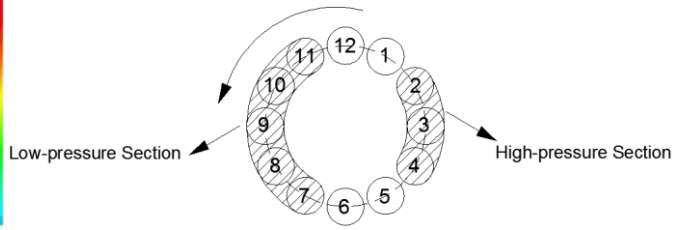
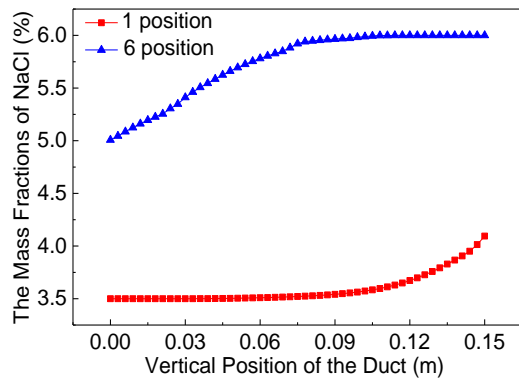
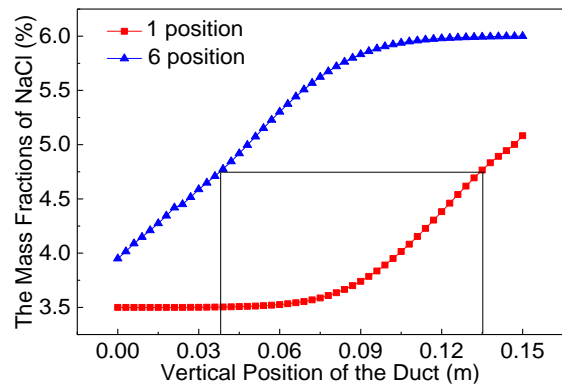


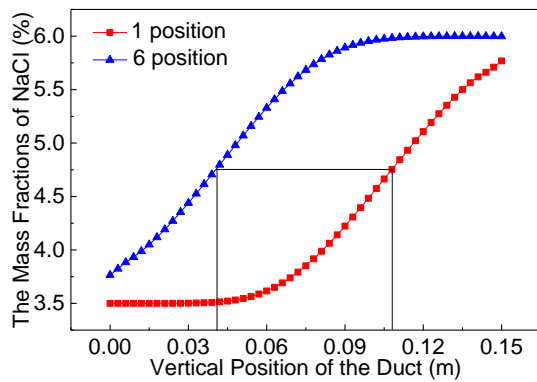
Figure 3: Arrange distribution of ducts on the rotor.



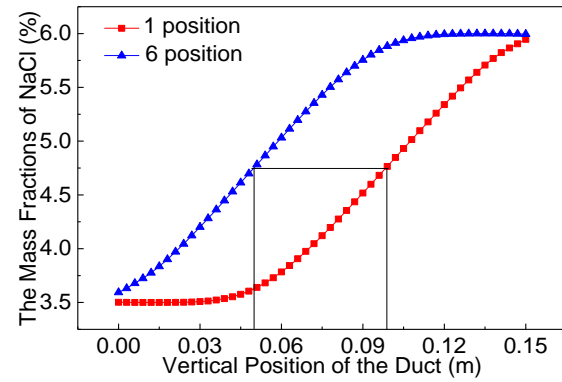
(a)



(b)



(c)



(d)

Figure 4: NaCl distributions along the vertical position of the duct. a) rotor speed 600 rpm; b) rotor speed 900 rpm; c) rotor speed 1,200 rpm; d) rotor speed 1,500 rpm.

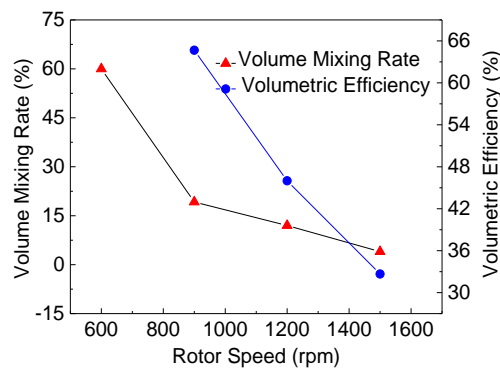


Figure 5: The relationships of the volume mixing rate, the volumetric efficiency and the rotor speed.

3.3 Effect of flow velocity on volume mixing rate and volumetric efficiency.

Figure 6 shows the NaCl distributions at the same rotor speed of 1,200 rpm under different flow velocities. It can be seen that when the rotor speed is the same, the contact time between the end cover and the rotor are same. The decreasing of the flow velocity leads the inlet flow to reduce at the same period of time, so that the maximum inflow length decreases. By changing the flow velocity to explore the performance of RPE, the main parameters also include the maximum flow length, the volume mixing rate and the volumetric efficiency, as presented in Table 2. When the rotor speed decreases, it can lead to the different decreasing behaviors of the volume mixing rate and the volumetric efficiency.

Table 2: Main performance parameters of RPE with different flow velocities.

Flow velocity (m/s)	Maximum inflow length (m)	Volume mixing rate (%)	Volumetric efficiency (%)
1.5	0.041	6	27.33
2	0.049	8.7	32.67
2.5	0.055	9.6	36.67
3	0.07	12	46

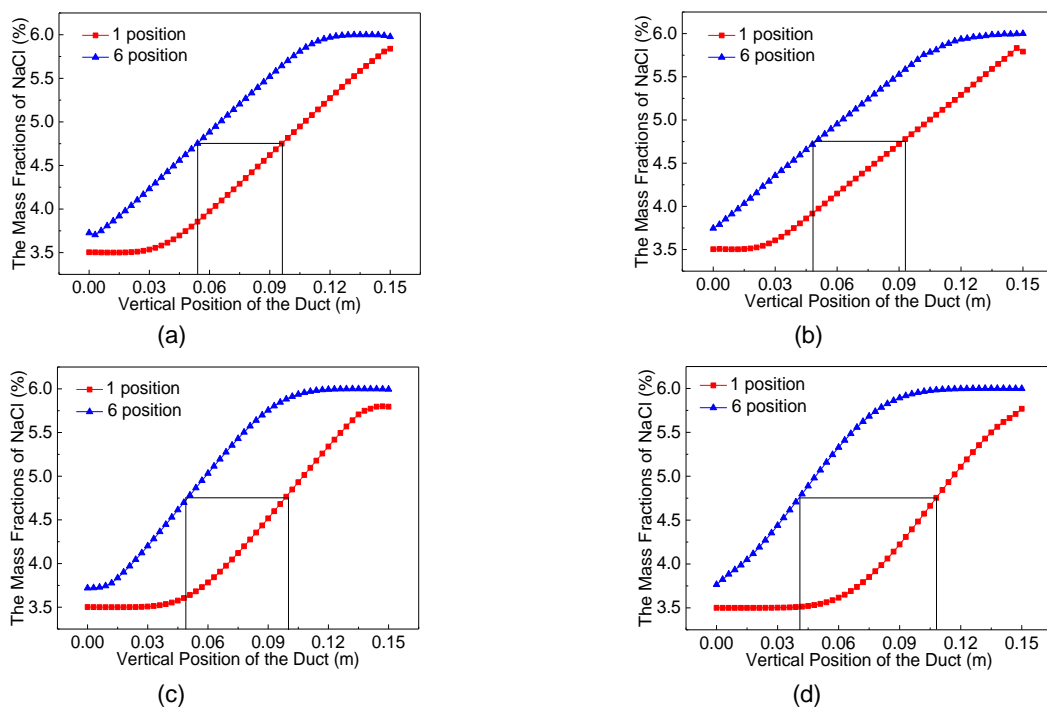


Figure 6: NaCl distributions along the vertical position of the duct. (a) flow velocity 1.5 m/s (b) flow velocity 2 m/s (c) flow velocity 2.5 m/s (d) flow velocity 3 m/s.

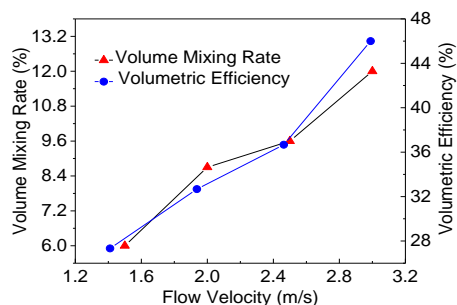


Figure 7: The relationships of the volume mixing rate the volumetric efficiency and the flow velocity.

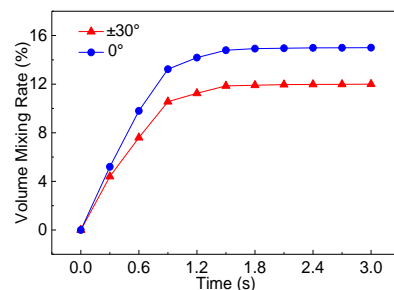


Figure 8: The relationship of volume mixing rate and the extended angle.

The relationships of the volume mixing, the volumetric efficiency and the flow velocity are shown in Figure 7. It can be seen that the flow velocity is proportional to the volume mixing rate and volumetric efficiency. As the flow velocity increases, the volumetric efficiency also increases. However, the flow velocity can not be increased without limit. When the flow velocity is too large, which can lead to the mixing zone overflow, and the quality of high-pressure export seawater can be influenced.

3.4 Effect of the extended angle on volume mixing rate

Figure 8 shows the relationship of volume mixing rate and the extended angle. The models of $\pm 30^\circ$ and 0° have the same trend when forming a stable blending zone. Before time of 1.5, the slope of the curve is large, indicating that the mixing occurs when the two fluids are in contact. After a certain period of time, a stable mixing zone is formed, and the volume mixing rate is maintained within a certain range. The volume mixing rate of $\pm 30^\circ$ is lower than the model without extended angle. It means that increasing the extended angle is beneficial to the formation of a lower volume mixing rate.

4. Conclusion

In this paper, based on the asymmetric model, the influences of the extended angle of the end cover structure on the volume mixing rate and the volumetric efficiency were studied by changing the extended angle of the end cover. The two end cover structures of extended angles of 0° , $\pm 30^\circ$ were designed. Moreover, the three-dimensional models were established. Different structure and operation parameters were taken into account to investigate the flow characteristics of the unsteady flow field and the development of high and low pressure fluid mixing properties in the rotor duct. The unsteady flow mechanism of RPE was revealed by analyzing the flow field. The simulation results show that the liquid piston moves cyclically. When the liquid piston is stable, the mass fractions of NaCl at high-pressure outlet will no longer change. When the flow velocity remains the same, the rotor speed is inversely proportional to the volume mixing rate and the volumetric efficiency. As the rotor speed increases, the volume mixing rate and volumetric efficiency decrease. When the rotor speed remains the same, the flow velocity is proportional to the volume mixing rate and the volumetric efficiency. As the flow velocity increases, the volume mixing rate and volumetric efficiency also increase. Therefore, it can be concluded that the model with the extended angle of $\pm 30^\circ$ has a smaller volume mixing rate. The results of this study provide a basis for the design and optimization of RPE, and also establish a theoretical guidance for controlling the hydraulic driven rotary device.

Acknowledgments

This work is supported by the National Natural Science Foundation of China (No.51306166).

References

- Cao Z., Deng J., Yuan W., Chen Z., 2016, Integration of CFD and RTD analysis in flow pattern and mixing behavior of rotary pressure exchanger with extended angle, *Desalination and Water Treatment*, 57, 15265-15275.
- Elimelech M., Phillip W. A., 2011, The future of seawater desalination: energy, technology, and the environment, *science*, 333, 712-717.
- Liu Y., Zhou Y. H., Bi M. S., 2012, 3D numerical simulation on mixing process in ducts of rotary pressure exchanger, *Desalination and Water Treatment*, 42, 269-273.
- Mei C. C., Liu Y. H., Law A. W., 2012, Theory of isobaric pressure exchanger for desalination. *Desalination and Water Treatment*, 39(1-3), 112-122.
- Stover R L., 2004, Development of a fourth generation energy recovery device. A 'CTO's notebook'. *Desalination*, 165, 313-321.
- Tamburini A., Giacalone F., Cipollina A., Grisafi F., Vella G., Micale G., 2016, Pressure Retarded Osmosis: a Membrane Process for Environmental Sustainability, *Chemical Engineering Transactions*, 47, 355-360.
- Wang Y., Wu L., Li B., Zhang W., Hu Y., 2016, Numerical Simulation and Analysis of the Mixing Process of Rotary Pressure Exchangers with Different Sizes and Structures, *Journal of Chemical Engineering of Japan*, 49, 573-578.
- Wu L., Wang Y., Xu E., Wu J., Xu S., 2015, Employing groove-textured surface to improve operational performance of rotary energy recovery device in membrane desalination system, *Desalination*, 369, 91-96.
- Xu E., Wang Y., Wu L., Xu S., Wang Y., Wang S., 2014, Computational Fluid Dynamics Simulation of Brine–Seawater Mixing in a Rotary Energy Recovery Device, *Industrial & Engineering Chemistry Research*, 53, 18304-18310.
- Zhou Y. H., Ding X. W., Ju M. W., Chang Y. Q., 2009, Numerical simulation on a dynamic mixing process in ducts of a rotary pressure exchanger for SWRO, *Desalination and Water Treatment*, 1, 107-113.